Chapter 29

Development of ATP-Competitive mTOR Inhibitors

Qingsong Liu, Seong A. Kang, Carson C. Thoreen, Wooyoung Hur, Jinhua Wang, Jae Won Chang, Andrew Markhard, Jianming Zhang, Taebo Sim, David M. Sabatini, and Nathanael S. Gray

Abstract

The mammalian Target of Rapamycin (mTOR)-mediated signaling transduction pathway has been observed to be deregulated in a wide variety of cancer and metabolic diseases. Despite extensive clinical development efforts, the well-known allosteric mTOR inhibitor rapamycin and structurally related rapalogs have failed to show significant single-agent antitumor efficacy in most types of cancer. This limited clinical success may be due to the inability of the rapalogs to maintain a complete blockade mTOR-mediated signaling. Therefore, numerous efforts have been initiated to develop ATP-competitive mTOR inhibitors that would block both mTORC1 and mTORC2 complex activity. Here, we describe our experimental approaches to develop Torin1 using a medium throughput cell-based screening assay and structure-guided drug design.

Key words: mTOR, mTORC1, mTORC2, PI3K, PIKK, Akt, Rapamycin, Torin1

1. Introduction

mTOR (mammalian Target of Rapamycin) is a serine/threonine protein kinase that is highly conserved across eukaryotes. It plays a critical role in the regulation of fundamental cellular physiological processes in response to the upstream cellular signals such as growth factors, energy, stress, and nutrient to control cell growth, proliferation, and metabolism through two known complexes, namely, mTORC1 and mTORC2 (1). mTORC1 is a primary regulator of protein translation through the phosphorylation of the S6 kinase and the inhibitory 4E-binding proteins (4EBPs). mTORC2 phosphorylates and regulates Akt, a downstream effector of the PI3K

Thomas Weichhart (ed.), *mTOR: Methods and Protocols*, Methods in Molecular Biology, vol. 821,
DOI 10.1007/978-1-61779-430-8_29,

signaling pathway that mediates growth and survival signals. Rapamycin, an allosteric inhibitor of mTOR that was originally identified as an immunosuppressant and later as an anticancer agent, has greatly facilitated the study of mTOR signaling (2, 3). As a key node in the oncogenic phosphoinositide 3-kinase signaling pathway, deregulation of the mTOR kinase has been often observed in human cancers (4–6). Inspired by the promising *in vitro* anticancer effect, it is widely believed that rapamycin or related analogs (rapalogs) would be therapeutically effective by blocking the mTORC1's phosphorylation activity of S6K and 4EBPs, which are key upstream regulators of protein synthesis. However, extensive clinical evaluation has found rapamycin's *in vivo* efficacy to be limited to a few rare cancers, such as renal cell carcinoma and mantle cell lymphoma (7). This may be partially explained by the recent discovery that rapamycin could not block the function of mTORC1 completely and has little effect on mTORC2 complex in the majority of cell types (4, 8). Moreover, the existence of a feedback loop that hyperactivates PI3K when mTORC1 is inhibited (9) and the recent discovery that rapamycin fails to completely inhibit mTORC1 indicates that ATP-competitive small molecule mTOR inhibitors might show broader efficacy.

Structurally, the mTOR catalytic domain exhibits high sequence identity with PI3Ks and PI3K-related kinases (PIKK) such as ATR, ATM, DNA-PK, and SMG-1. The co-crystal structure of LY294002 with PI3Kγ provides valuable insights that enable structure-guided design of numerous PI3K inhibitors (10). The dual PI3K/mTOR inhibitor PI-103, similar to LY294002, which uses the morpholine oxygen as the hinge binding moiety, provides a molecular-entry point for the development of selective mTOR inhibitors (11, 12). For example, PI-103 served as a "lead" compound for the structure-guided development of selective mTOR inhibitors such as KU-0063794 (13) and WYE-354 (14) and other related structures (15) using a rational designed approach (Fig. 1). Preliminary biochemical analyses indicate that these compounds are, indeed, promising candidates for replacing rapamycin as future anticancer agents. Not only do these pharmacological inhibitors have enhanced efficacy in suppressing hyperactive mTOR, but also they are highly

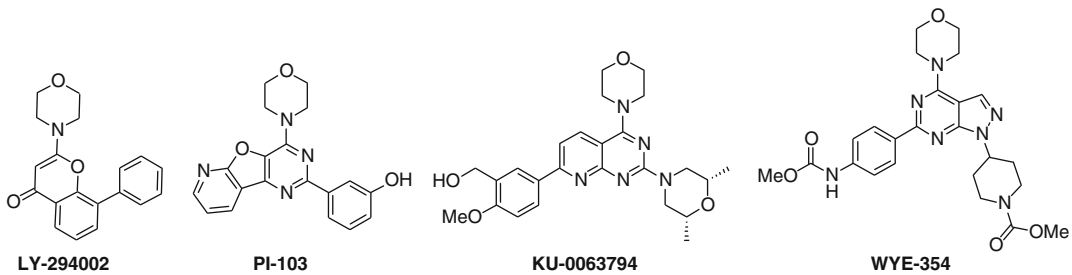

Fig. 1. Structures of PI3K and mTOR inhibitors.

specific in targeting mTOR in a large panel of cancer cell lines. More interestingly, these compounds inhibit the proliferation of diseased cells to a greater extent than rapamycin by targeting the rapamycin-insensitive mTOR complex in addition to the rapamycin-sensitive mTOR complex. We utilized a complementary approach to develop mTOR selective inhibitors which consisted of using medium-throughput biochemical screening of an ATP-site directed heterocyclic compound library followed by iterative-chemical synthesis guided by cell-based SAR analysis and molecular modeling .

2. Materials

2.1. Chemical Synthesis Materials

1. All commercially available chemical materials were used directly without further purification.

2.2. Cell Culture and Lysis

1. Cell culture media: DMEM, 10% fetal bovine serum, penicillin/streptomycin (Invitrogen, Carlsbad, CA).
2. Centrifuge: RC-5 C plus (Sorvall).

2.3. SDS-Polyacrylamide Gel Electrophoresis

1. SDS-Polyacrylamide gel: NuPAGE 4–12% Bis–Tris Gel 1.5 mm, 15 well (Invitrogen, Carlsbad, CA).
2. Running buffer (20×): NuPAGE MES SDS running buffer or NuPAGE MOPS SDS running buffer (Invitrogen, Carlsbad, CA).

2.4. Western Blotting for Active S6K1 and Akt

1. Transfer buffer: 10 mM CAPS, 10% (v/v) ethanol.
2. Immobilon-P transfer membrane from Millipore, Bedford, MA, and 3MM Chr chromatography paper from Whatman, Maidstone, UK.
3. Phosphate-buffered saline with Tween (PBS-T): 0.137 M NaCl, 2.7 mM KCl, 10.0 mM Na_2HPO_4, 1.76 mM KH_2PO_4, pH 7.4, 0.1% Tween-20.
4. Blocking buffer: 5% (w/v) nonfat dry milk in PBS-T.
5. Primary antibody dilution buffer: PBS-T supplemented with 5% (w/v) bovine serum albumin (BSA).
6. Primary antibodies: Phospho-S6K1 (Thr-389) and phospho-Akt (Ser-473) (Cell Signaling Technology, Danvers, MA).
7. Secondary antibody: Anti-mouse IgG (for phospho-S6K1) and anti-rabbit IgG (phospho-Akt) conjugated to horse radish peroxidase (Santa Cruz Biotechnology, Santa Cruz, CA).
8. Enhanced chemiluminescent (ECL) reagent: Western Lighting–ECL (Perkin Elmer, Waltham, MA).

2.5. Material in U87MG Model Anti-Tumor Study

1. Immunodeficient mice: NCR nude, nu/nu (Taconic Laboratories).
2. Drug vehicle: 20%:40%:40% (v/v) *N*-methyl-2-pyrrolidone: PEG400:water.

3. Methods

3.1. Overview of the Process

As illustrated in Fig. 2, the workflow for developing potent and selective mTOR inhibitors commenced with a medium-throughput biochemical screening of a focused ATP-site directed heterocycle library. Compounds that exhibited activity in this assay were then profiled for selectivity across a panel of approximately 400 kinases using the Ambit KinomeScan methodology from which a class of quinoline-derived compounds appeared to exhibit the greatest selectivity for mTOR. Compounds were then evaluated for their ability to inhibit the downstream target of mTORC1 S6K T389 in a cellular assay utilizing mouse embryonic fibroblasts (MEFs). A key goal of this project was to identify compounds that exhibited selectivity for inhibition of mTOR relative to structurally homologous PIKK family members such as the PI3Ks. The ability of the compounds to inhibit PI3K was evaluated by measuring effects on the activation loop phosphorylation site of Akt T308 in the context of the S473D mutant form of Akt in PC-3 cells. The S473D mutant of Akt was employed because this "phospho-mimetic" mutation abolishes the effects that would result from mTORC2-mediated phosphorylation

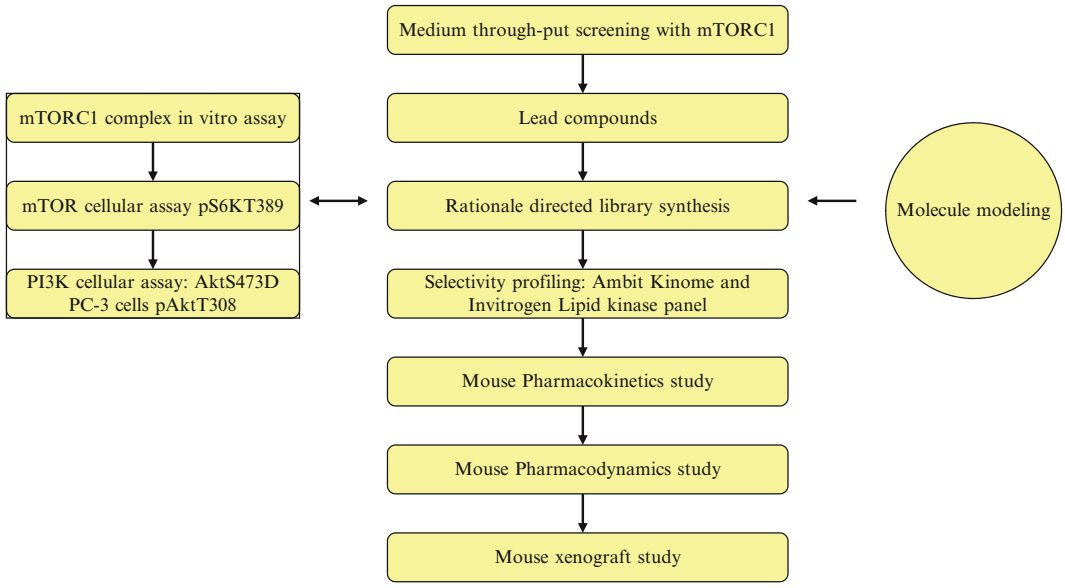

Fig. 2. Flowchart for developing mTOR inhibitors.

of this site (8). This is a necessary precaution because most inhibitors in our series are very potent inhibitors of mTORC2 and this would confound our ability to evaluate how potent they are as inhibitors of PI3K. The structure–activity relationships derived from these cellular assays was interpreted in the context of a molecular model for the presumed binding mode. A homology model of the three-dimensional structure of mTOR was constructed using Autodock Vina. This information was then used to inform the design of iterative rounds of compound synthesis. Given the fairly challenging nature of the chemistry required to prepare these compounds, we were never able to prepare focused libraries of derivatives. The most potent and selective compounds were subjected to broader selectivity profiling across a panel of approximately 450 kinases using the Ambit KinomeScan™ technology. The selected compounds chosen from this profiling were then tested in Invitrogen SelectScreen® lipid kinase panel including all of the PI3K isomers and DNA-PK. The most selective compounds were subject to metabolic stability studies using isolated mouse microsomes and then evaluated in mice for their pharmacokinetic and pharmacodynamic properties. Candidate compounds were then tested for antitumor efficacy using mouse tumor xenograft models.

3.2. Chemical Synthesis Methodology

1. Combinatorial kinase-directed libraries were built from a variety of commercially available heterocycles using both solution and solid phase synthesis (16). Simple and robust chemistries such as nucleophilic aromatic substitution and palladium-mediated couplings were used to install diverse elements. For example, disubstituted quinazolines were constructed starting from compound **1** (4,6-dichloroquinazoline) using a nucleophilic substitution reaction to install a particular aniline to the *C4* position followed by a Suzuki coupling reaction to install an aromatic side chain to the *C6* position of the quinazoline (Scheme 1).

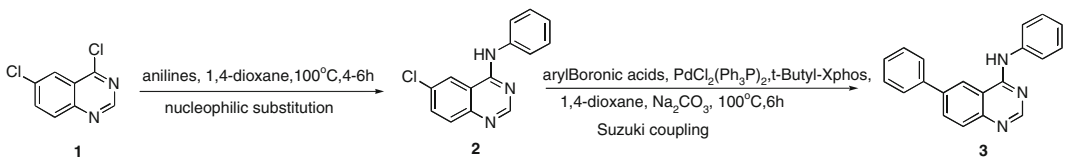

Scheme 1. Synthesis of the high-throughput library.

2. Rationally designed focused library synthesis was accomplished using the synthetic scheme exemplified in Scheme 2 (17). Compound **4** (Ethyl-4,6-dichloroquinoline-3-carboxylate) was subjected to nucleophilic addition by particular aryl anilines to afford compound **5** (Scheme 2). Lithium aluminum hydride (LAH)-mediated reduction of the ethyl ester furnished the corresponding benzyl alcohol compound **6**. Benzylic oxidation

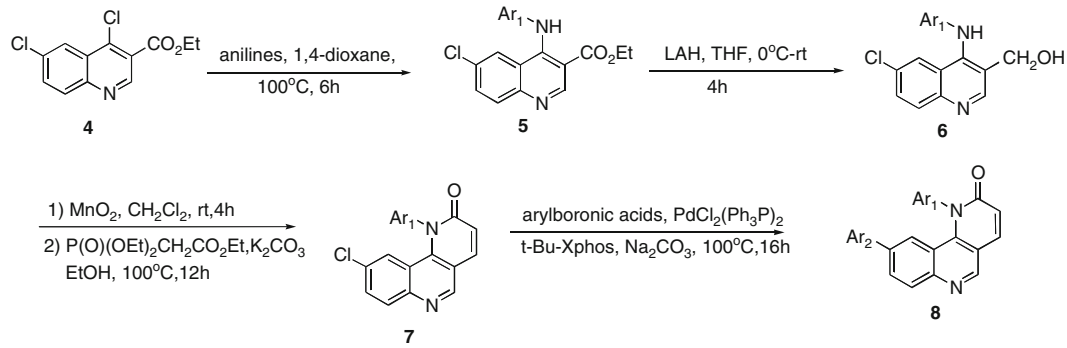

Scheme 2. Synthesis of the focused library.

with MnO_2 followed by Horner–Emmons–Wardsworth olefination generated the cyclized compound **7**. Finally, a Suzuki coupling reaction was used to install an additional aryl side chain at *C6* position of the quinoline.

A detailed synthetic protocol is provided below:

(a) To a solution of compound **4** (1 equiv.) in 1,4-dioxane was added aniline (1–2 equiv.) at room temperature. The reaction mixture was then heated to 100°C for 4–6 h and then allowed to cool to room temperature. An aqueous NaOH (1N) solution was added to neutralize the reaction mixture. The resultant solution was diluted with water and extracted with ethyl acetate. After the removal of the solvents under vacuum, the residue was purified by flash column chromatography (hexanes/EtOAc) to afford compound **5** (see Note 1).

(b) To a solution of compound **5** (1 equiv.) in THF at 0°C was added LAH (3–5 equiv.) dropwise. After 15–20 min, the solution was warmed to room temperature and stirred for 1–4 h before carefully quenching with methanol and water. Dilution of the mixture with EtOAc and filtration through celite furnished crude **6**, which was used in the next step without further purification (see Note 2).

(c) To a solution of compound **6** in CH_2Cl_2 (1 equiv.) at room temperature was added MnO_2 (10 equiv. mass). After 1–4 h, the reaction mixture was filtered through celite. The filtrate was concentrated and placed in a sealed tube and dissolved in dry EtOH. K_2CO_3 (3 equiv.) and triethyl phosphonoacetate were then added sequentially. The resulting mixture was heated to 100°C for 12–16 h before cooling to room temperature. Upon removal of the solvents under vacuum, the residue was diluted with water followed by extraction with ethyl acetate (3×). Purification of the residue by flash column chromatography (hexanes/EtOAc) provided compound **7** (see Note 3).

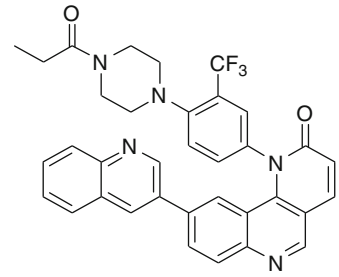

Fig. 3. Structure of Torin1.

(d) To a solution of compound 7 in 1,4-dioxane at room temperature was added subsequently $PdCl_2(Ph_3P)_2$ (0.1 equiv.), *t*-Bu-Xphos (0.1 equiv.), Na_2CO_3 (3 equiv., 1N) and boronic acids or pinacol boronic esters. After degassing, the resultant mixture was heated to 100°C for 6 h before cooling to room temperature and filtering through celite. Upon removal of the solvents, the residue was subjected to column chromatography purification (hexanes/EtOAc) to furnish the desired compounds as exemplified by compound **8** (see Note 4). The structure of Torin1 generated following above procedures was shown in Fig. 3.

3.3. Biochemical Assay of mTORC1 Complex

3.3.1. Preparation of Human Soluble mTORC1 Complex

1. HEK-293T cells that stably expressed N-terminally FLAG-tagged raptor using vesicular stomatitis virus G-pseudotyped MSCV retrovirus was used as a source of mTORC1 complex.
2. The HEK293T cells were lysed in 50 mM HEPES, pH 7.4, 150 mM NaCl, and 0.4% CHAPS at 4°C for 30 min, and the insoluble fraction was removed by centrifugation at 39,000 G for 30 min. Supernatants were incubated with FLAG-M2 monoclonal antibody-conjugated agarose for 1 h and then washed with two column volumes of wash buffer 1 (50 mM HEPES, pH 7.4, 150 mM NaCl, 2 mM DTT and 2 mM ATP, and 0.1% CHAPS) and another two column volumes of wash buffer 2 (50 mM HEPES, pH 7.4, 200 mM NaCl, and 0.1% CHAPS).
3. mTORC1 complex was eluted with 100 μg/ml 3× FLAG peptide in 50 mM HEPES, pH 7.4, 500 mM NaCl, and 0.1% CHAPS, then concentrated by centrifugation. Pure mTORC1 was isolated after gel filtration using a tandem Superose 6 10/300 GL column (GE Healthcare) in 50 mM HEPES, pH 7.4 and 150 mM NaCl on an AKTA purifier (GE Healthcare).

3.3.2. In Vitro mTORC1 Activity Assay (Lanthascreen™ Time-Resolved FRET Assay)

1. mTORC1 (0.1 μg each) was incubated with serially diluted inhibitors (threefold, 11 points) for 30 min in 5 μl kinase buffer (25 mM HEPES, pH 7.4, 10 mM $MgCl_2$, 4 mM $MnCl_2$, 50 mM KCl) in a 384-well low volume plate (Corning).

2. The kinase reaction was initiated by the addition of an equal volume of kinase buffer containing 0.8 μM GFP-labeled 4E-BP1 and 100 μM ATP at room temperature. After the kinase reaction for 1 h, the reaction was stopped by the addition of 10 μl of solution containing 20 mM EDTA and 4 nM Tb-labeled antiphospho 4E-BP1 (T46) antibody (Invitrogen).
3. After incubation for 30 min, the FRET signal between Tb and GFP within the immune complex was read using Envision plate reader (PerkinElmer). Each data point was duplicated and IC_{50} values were calculated using Prism4 software (GraphPad).

3.4. Cellular Assays of mTOR and PI3K Activities

1. Cell Lysis: Cells were rinsed once with ice-cold PBS and lysed in an ice-cold lysis buffer (40 mM HEPES, pH 7.4, 2 mM EDTA, 10 mM pyrophosphate, 10 mM glycerophosphate, and 0.3% CHAPS or 1% Triton X-100, and one tablet of EDTA-free protease inhibitors per 25 ml). The soluble fractions of cell lysates were isolated by centrifugation at 13,000 rpm for 10 min in a microcentrifuge (18).
2. Cellular IC_{50} values for mTOR were determined using $p53^{-/-}$ MEFs. Cells were treated with vehicle or increasing concentrations of compound for 1 h and then lysed. Phosphorylation of S6K1 Thr-389 was monitored by immunoblotting using a phospho-specific antibody.
3. Cellular IC_{50} values for PI3K were determined using $p53^{-/-}$/$mLST8^{-/-}$ MEFs. Cells were treated with vehicle or increasing concentrations of compound for 1 h and then lysed. Phosphorylation of Akt Thr-308 was monitored by immunoblotting using a phospho-specific antibody. The summary of Torin1's biochemical and cellular IC_{50}s was shown in Table 1.

3.5. Molecular Modeling

An mTOR homology model was built with Modeller(9v6) based on a published PI3Kγ crystal structure complexed with GDC-0941 (PDB: 3DBS). Compounds were docked into the model with Autodock Vina (19). The presumed proper binding conformation was selected based on the binding modes of structurally related inhibitors whose co-structures had been determined crystallographically. An example of the docking result of Torin1 with mTOR complex was shown in Fig. 4.

Table 1
Biological evaluation summary of Torin1

Recombinant mTOR biochemical assay IC_{50} (nM)	mTORC1 *in vitro* assay IC_{50} (nM)	mTOR in cellular assay IC_{50} (nM)	PI3K in cellular assay IC_{50} (nM)
4	0.29	2	1800

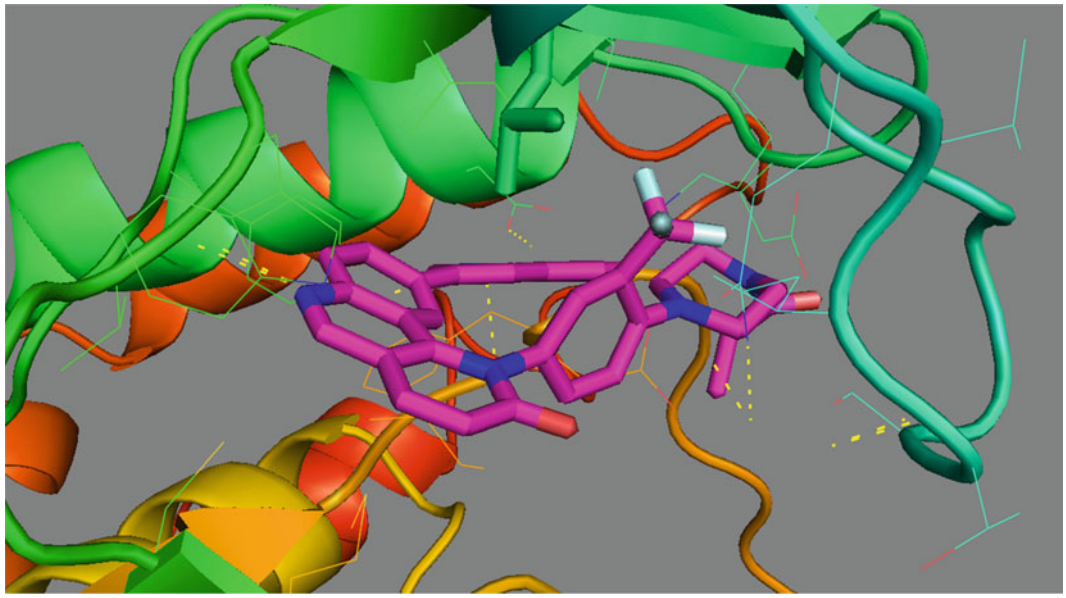

Fig. 4. Torin1 was docked into homology modeled mTOR 3D structure.

3.6. Ambit Kinome Wide and Invitrogen Lipid Kinase Panel Selectivity Profiling

1. Ambit kinome wide selectivity profile was performed in Ambit Bioscience with KinomeScan™ technology. Interesting compounds were profiled at a concentration of 10 μM against a diverse panel of 442 kinases by Ambit Biosciences. Scores for primary screen hits are reported as a percent of the DMSO control (% control). For kinases where no score is shown, no measurable binding was detected. The lower the score, the lower the Kd is likely to be, such that scores of zero represent strong hits. Scores are related to the probability of a hit, but are not strictly an affinity measurement. At a screening concentration of 10 μM, a score of less than 10% implies that the false-positive probability is less than 20% and the Kd is most likely less than 1 μM. A score between 1 and 10% implies that the false-positive probability is less than 10%, although it is impossible to assign a quantitative affinity from a single-point primary screen. A score of less than 1% implies that the false-positive probability is less than 5% and the Kd is most likely less than 1 μM.
2. Invitrogen lipid kinase panel profile was conducted in LifeScience Inc. using SelectScreen® technology by testing IC_{50} on individual kinase with ten testing points from a starting 1 μM drug concentration. PIKK family kinase profiling result of Torin1 in Ambit and Invitrogen was shown in Table 2.

3.7. Pharmacokinetic Studies

1. The study was performed in Sai Advantium Pharma Limited Company (India) with male Swiss Albino mice following single intravenous bolus, oral administration, and intraperitoneal injection.

Table 2
Summary of Ambit and Invitrogen selectivity profiles of PIKK-family kinases

Kinase entry	Ambit score	Invitrogen IC_{50} (nM)	Kinase entry	Ambit score	Invitrogen IC_{50} (nM)
PIK3C2B	25	549	PIK3CA(I800L)	0	ND
PIK3C2G	11	ND	PIK3CA(M1043I)	8.6	ND
PIK3CA	1.3	250	PIK3CA(Q546K)	6.8	ND
PIK3CA(C420R)	0.7	ND	PIK3CB	65	ND
PIK3CA(E542K)	1	ND	PIK3CD	51	564
PIK3CA(E545A)	1	ND	PIK3CG	1.2	171
PIK3CA(E545K)	0.6	ND	PIK4CB	96	6,680
PIK3CA(H1047L)	2.6	ND	DNA-PK	ND	6.34
PIK3CA(H1047Y)	12	ND	mTOR	0	4.32

2. Nine mice were injected 1 mg/kg of Torin1 solution (10% v/v *N*-methyl pyrrolidone and 50% v/v polyethylene glycol-200 in normal saline) via tail vein. Blood samples were collected at 0, 0.08, 0.25, 0.5, 1, 2, 4, and 6 h (see Note 5).
3. Nine mice were dosed orally 10 mg/kg of Torin1 suspension (0.5% w/v Na CMC with 0.1% v/v Tween-80 in water). Blood samples were collected at 0, 0.08, 0.25, 0.5, 1, 2, 4, 6, 8, 12, and 24 h (see Note 5).
4. Nine mice were injected 10 mg/kg of Torin1 solution (10% v/v *N*-methyl pyrrolidone and 20% v/v polyethylene glycol-200 in normal saline and 20% PG in water) via peritoneum. Blood samples were collected at 0, 0.08, 0.25, 0.5, 1, 2, 4, 8, and 24 h (see Note 6).
5. All samples were processed for analysis by precipitation using acetonitrile and analyzed with a partially validated LC/MS/MS method (LLOQ – 1.138 ng/ml). Pharmacokinetic parameters were calculated using the noncompartmental analysis tool of WinNonlin® Enterprise software (version 5.2). The I.V., P.O., and I.P. studies of Torin1 were summarized in Table 3.

3.8. Pharmacodynamic Studies

1. Torin1 was formulated by dissolving the compound at a concentration of 25 mg/ml in 100% *N*-methyl-2-pyrrolidone followed by dilution (1:4) with sterile 50% PEG-400 prior to injection.
2. Six-week-old male C57BL/6 mice were fasted overnight prior to drug treatment. The mice were treated with vehicle (for 10 h) or Torin1 (20 mg/kg for 2, 6, or 10 h) by IP injection, and then refed 1 h prior to sacrifice (CO_2 asphyxiation).

Table 3
Summary of pharmacokinetic test (reproduced from ref. 17)

Route	C_{max} (ng/ml)	T_{max} (h)	AUC (h ng/ml)	$T_{1/2}$ (h)	MRT (h)	CL (ml/min/kg)	V_{ss} (l/kg)	F (%)
I.V.	2,757	ND	720	0.5	0.43	23.0	0.59	ND
P.O.	223	0.25	396	0.79	1.51	ND	ND	5.49
I.P.	5,121	0.08	5,718	4.52	ND	ND	ND	ND

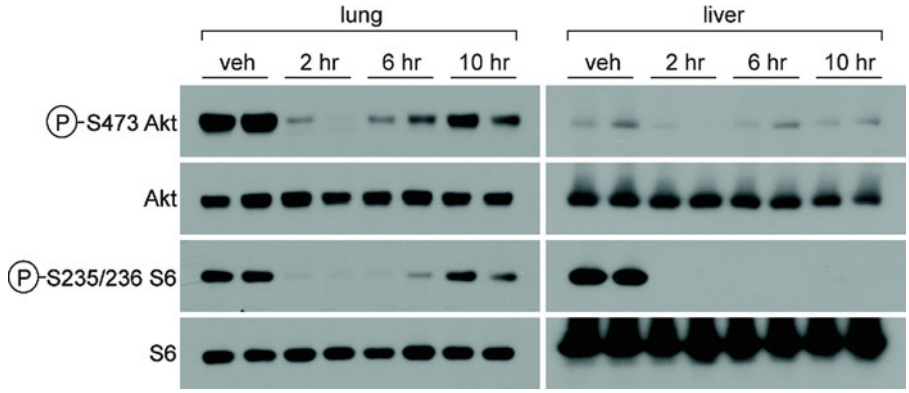

Fig. 5. Pharmacodynamic study of Torin1 (reproduced from ref. 17).

3. Tissues were collected and frozen on dry ice. The frozen tissue was thawed on ice and lysed by sonication in tissue lysis buffer (50 mM HEPES, pH 7.4, 40 mM NaCl, 2 mM EDTA, 1.5 mM sodium orthovanadate, 50 mM sodium fluoride, 10 mM sodium pyrophosphate, 10 mM sodium β-glycerophosphate, 0.1% SDS, 1.0% sodium deoxycholate, and 1.0% Triton, supplemented with protease inhibitor cocktail tablets [Roche]).
4. The concentration of clear lysate was measured using the Bradford assay and samples were subsequently normalized by protein content and analyzed by SDS-polyacrylamide gel electrophoresis (SDS-PAGE) and immunoblotting. The result of PD study of Torin1 was exemplified in Fig. 5.

3.9. Animal Xenograft Study (U87 Model)

1. 2×10^6 U87MG glioblastoma cells were resuspended in 100 μl of media that had been premixed with matrigel, and was injected subcutaneously in the upper flank region of mice (6 weeks old immunodeficient) that had been anesthetized with isoflurane. Tumors were allowed to grow to 1 cm^3 in size (see Note 6).
2. Animals were divided into two treatment groups randomly for vehicle and Torin1. Torin1 was formulated as 5 mg/ml in a solution of *N*-methyl-2-pyrrolidone:PEG400:water

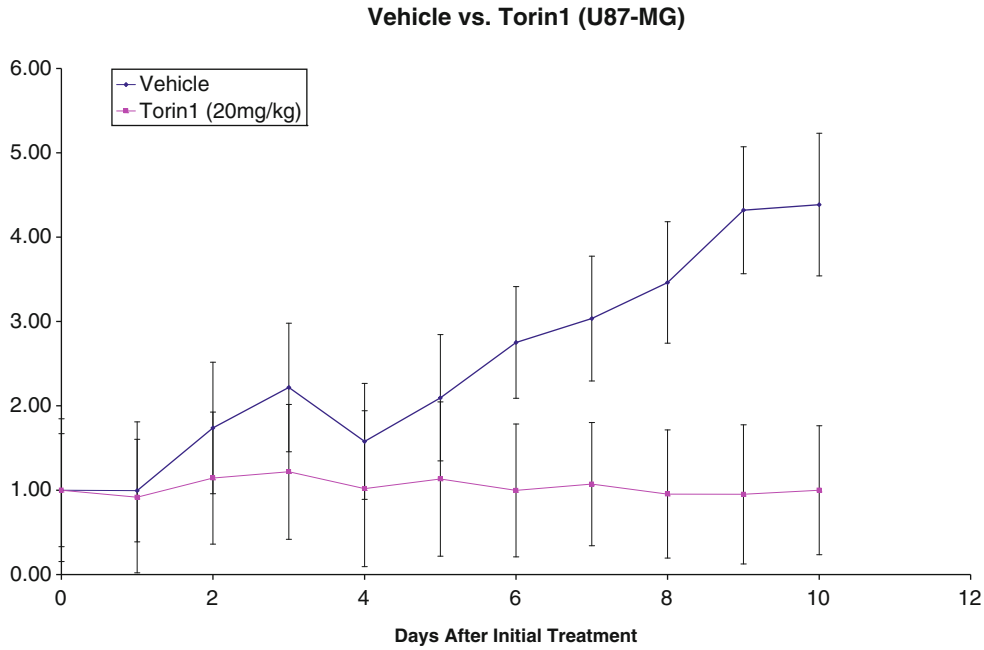

Fig. 6. U87MG tumor xenograft model study of Torin1 (reproduced from ref. 17).

(20%: 40%:40%). Both vehicle and Torin1 were delivered by IP injection at a dosage of 20 mg/kg (q.d.)

3. Tumors were measured with calipers in two dimensions every other day. Tumor volumes were estimated with the formula: volume = $(2a \times b)/2$, where a = short and b = long tumor axes, respectively, in millimeters. The result of Torin1's antitumor activity was exhibited in Fig. 6.

4. Notes

1. Some series of compound **5** would require $CHCl_3$/iPrOH (4:1) extraction system due to a poor solubility in EtOAC.
2. LAH should be added at 0°C to avoid facile over reduction of the benzyl alcohol to the toluene-like product. The reaction is typically monitored carefully by LC-MS to avoid over reduction after warming up to room temperature. A 0°C ice-water bath is preferred during the quenching procedure and the methanol should be added drop-wise due to the exothermic reaction. Extra EtOAc would be used to rinse the filtrate to avoid loss of the product in the celite.
3. Complete removal of the EtOH under vacuum is needed to avoid complications with the purification process.

4. Some compound **8** analogs are very polar and require reverse phase column chromatography with MeOH/water or CH_3CN/water solvent system.
5. All blood samples were collected in microcentrifuge tubes containing K2EDTA as an anticoagulant. At each time point, plasma samples from a set of three mice were separated by centrifugation and stored below –70°C until bioanalysis.
6. Immunodeficient mice (NCR nude, nu/nu; Taconic Laboratories) were maintained in a pathogen-free facility and were given autoclaved food and water ad libitum. All animal studies were performed according to the official guidelines from the MIT Committee on Animal Care and the American Association of Laboratory Animal Care.

Acknowledgements

We thank Life Technologies Corporation for SelectScreen® Kinase Profiling Service and Ambit Bioscience for performing KinomeScan™ profiling. We also thank SAI Advantium Pharma Limited Inc. (India) for the pharmacokinetic study.

References

1. Sarbassov, D. D., Ali, S. M., Sabatini, D. M. (2005) Growing roles for the mTOR pathway. *Curr. Opin. Cell Biol.* **17**, 596–603.
2. Sehgal, S. N.; Baker, H.; Vezina, C. (1975) Rapamycin (AY-22989), a new antifungal antibiotic. II. Fermentation, isolation and characterization. *J. antibiotics (Tokyo)*, **28**, 727–732.
3. Rao, R. D.; Buckner, J. C.; Sarkaria, J. N. (2004) mammalian Target of Rapamycin (mTOR) Inhibitors as Anti-Cancer Agents. *Curr. Cancer Drug. Targets.* **4**, 621–635.
4. Guertin, D. A., Sabatini, D.M. (2007) Defining the role of mTOR in cancer. *Cancer cell*, **12**, 9–22.
5. Molinolo, A. A., Hewitt, S. M., Amornphimoltham, P., Keelawat, S., Rangdaeng, S., Meneses , A. et al (2007) Dissecting the Akt/ mammalian target of rapamycin signaling network: emerging results from the head and neck cancer tissue array initiative. *Clin Cancer Res,* **13**, 4964–4973.
6. Karbowniczek, M., Spittle, C.S., Morrison, T., Wu, H., Henske, E.P. (2008) mTOR is activated in the majority of malignant melanomas. *J Invest Dermatol* **128**, 980–987.
7. Meric-Bernstam, F., Gonzalez-Angulo, A. M. (2009) Targeting the mTOR signaling network for cancer therapy. *J Clin Oncol*, **27**, 2278–2287.
8. Thoreen, C. C., Kang, S. A., Chang, J. W., Liu, Q., Zhang, J., Gao, Y., et al. (2009) An ATP-competitive mammalian target of rapamycin inhibitor reveals rapamycin-insensitive functions of mTORC1. *J Biol Chem.* **284**, 8023–8032.
9. Wan, X., Harkavy, B., Shen, N., Grohar, P., Helman, L. J. (2007) Rapamycin induces feedback activation of Akt signaling through an IGF-1R-dependent mechanism. *Oncogene*, 26, 1932–1940.
10. Walker, E. H., Pacold, M. E., Perisic, O., Stephens, L., Hawkins, P. T., Wymann, M. P., et al. (2000) Structural determinants of phosphoinositide 3-kinase inhibition by wortmannin, LY294002, quercetin, myricetin, and staurosporine. *Mol. Cell*, **6**, 909–919.

11. Hayakawa, M., Kaizawa, H., Moritomo, H., Koizumi, T., Ohishi, T., Yamano, M., et al. (2007) Synthesis and biological evaluation of pyrido[3',2':4,5]furo[3,2-d]pyrimidine derivatives as novel PI3 kinase p110alpha inhibitors. *Bioorg. Med. Chem. Lett.*, 17, 2438–2442.
12. Park, S., Chapuis, N., Bardet, V., Tamburini, J., Gallay, N., Willems, L., et al. (2008) PI-103, a dual inhibitor of class IA phosphatidylinositide 3-kinase and mTOR, has antileukemic activity in AML. *Leukemia*, **22**, 1698–1706.
13. García-Martínez, J. M., Moran, J., Clarke, R. G., Gray, A., Cosulich, S. C., Chresta, C. M., et al. (2009) Ku-0063794 is a specific inhibitor of the mammalian target of rapamycin (mTOR). *Biochem J*, **421**, 29–42.
14. Yu, K., Toral-Barza, L., Shi, C., Zhang, W. G., Lucas, J., Shor, B., et al. (2009) Biochemical, cellular, and in vivo activity of novel ATP-competitive and selective inhibitors of the mammalian target of rapamycin. *Cancer Res.* **69**, 6232–6240.
15. Liu, Q., Thoreen, C. C., Wang, J., Sabatini, D. M., Gray, N. S. (2009) mTOR medicated anti-cancer drug discovery. *Drug. Discov. Today: Therapeutic Strategies.* **6**, 47–55.
16. Ding, S., Gray, N. S., Wu, X., Ding, Q., Schultz, P. G. (2002) A combinatorial scaf-fold approach toward kinase-directed heterocycle libraries. *J. Am. Chem. Soc.*, **124**, 1594–1596.
17. Liu, Q., Chang, J., Wang, J., Kang, S. A., Thoreen, C.C., Markhard, A., Hur, W., Zhang, J., Sim, T., Sabatini, D. M., Gray, N. S. (2010) Discovery of 1-(4-(4-propionylpiperazin-1-yl)-3-(trifluoromethyl)phenyl)-9-(quinolin-3-yl) benzo[h][1,6]naphthyridin-2(1 H)-one as a highly potent, selective mTOR inhibitor for the treatment of cancer. *J. Med. Chem.* DOI: 10.1021/jm101144f
18. Guertin, D. A., Stevens, D. M., Thoreen, C. C., Burds, A. A., Kalaany, N. Y., Moffat, J., Brown, M., Fitzgerald, K. J., Sabatini, D. M. (2006) Ablation in mice of the mTORC components *raptor*, *rictor*, or *mLST8* reveals that mTORC2 is required for signaling to Akt-FOXO and PKCalpha, but not S6K1. *Dev. Cell*, **11**, 859–871
19. Trott, O., Olson, A. J. (2010) Autodock vina: Improving the speed and accuracy of docking with a new scoring function, efficient optimization, and multithreading. *J. Comput. Chem.*, **31**, 455–461.